J. Fluid Mech. (1968), *vol.* 31, *part* 3, *pp.* 609–623
Printed in Great Britain

An experimental study of reverse transition in two-dimensional channel flow

By M. A. BADRI NARAYANAN
Department of Aeronautical Engineering,
Indian Institute of Science, Bangalore, India

(Received 10 December 1966 and in revised form 23 August 1967)

An experimental investigation on reverse transition from turbulent to laminar flow in a two-dimensional channel was carried out. The reverse transition occurred when Reynolds number of an initially turbulent flow was reduced below a certain value by widening the duct in the lateral direction. The experiments were conducted at Reynolds numbers of 625, 865, 980 and 1250 based on half the height of the channel and the average of the mean velocity. At all these Reynolds numbers the initially turbulent mean velocity profiles tend to become parabolic. The longitudinal and vertical velocity fluctuations ($\overline{u'^2}$ and $\overline{v'^2}$) averaged over the height of the channel decrease exponentially with distance downstream, but $\overline{u'v'}$ tends to become zero at a reasonably well-defined point. During reverse transition $\overline{u'v'}/\sqrt{\overline{u'^2}}\sqrt{\overline{v'^2}}$ also decreases as the flow moves downstream and Lissajous figures taken with u' and v' signals confirm this trend. There is approximate similarly between $\overline{u'^2}$ profiles if the value of $\overline{u'^2_{\max}}$ and the distance from the wall at which it occurs are taken as the reference scales. The spectrum of $\overline{u'^2}$ is almost similar at all stations and the non-dimensional spectrum is exponential in wave-number. All the turbulent quantities, when plotted in appropriate co-ordinates, indicate that there is a definite critical Reynolds number of 1400 ± 50 for reverse transition.

1. Introduction

The phenomenon of reverse transition from turbulent to laminar flow has been the object of study only recently, even though the transition from laminar to turbulent flow has been investigated to a considerable extent by many investigators. Reverse transition can be classified under the general topic 'the decay of turbulence' and in this field most investigations have been generally restricted so far to the case of isotropic turbulence (Batchelor 1959) where turbulent energy production is completely absent, which makes the analytical approach to the problem somewhat easier. On the other hand, the decay of non-isotropic turbulence, for example shear flows, is also of importance, but very little information is available on this subject. Our present-day knowledge even regarding the general nature of the process being poor, an analytical approach to this problem is not available and hence experimental investigations are necessary to understand the basic features of the reverse transition process.

Reverse transition in compressible boundary layers was observed some years ago by Sternberg (1954) and by Sergienko & Gretsov (1959). Holder, Gadd & Regan (1956) suspected decay of turbulence in the wake of a body at high Mach numbers. Recently, reverse transition has been reported by Launder (1964) and Moretti & Kays (1965) in accelerated incompressible turbulent boundary layers. In all these experiments the flows were subjected to large favourable pressure gradients associated with changes in Reynolds number.

In the present investigation, it was decided to study the reverse transition phenomenon in a simple and basic flow so that the gross features of the decay of non-isotropic turbulence could be understood. It has been observed that turbulence cannot persist below a certain Reynolds number for each particular type of flow, though the exact value has not yet been well established in all cases. The simplest set-up for this type of investigation is to decrease suddenly or gradually the Reynolds number of the flow which is initially turbulent and this condition can be easily achieved in a pipe or channel flow by increasing the area through a diffuser. In this way a large change in Reynolds number can be achieved in a pipe or channel flow depending on the area ratio of the diffuser and if the mass flow is properly controlled reverse transition can be achieved. A two-dimensional channel flow is more suitable for this investigation since measurements are somewhat easier in a channel than in a pipe. In the present case, the channel height was kept constant throughout its length and the width was increased through a diffuser to reduce the flow Reynolds number.

Some preliminary work of the same nature has been carried out independently by Laufer (1962) and Sibulkin (1962) in a pipe. Their experimental set-up was almost the same as that of the present investigation except that a pipe flow was chosen instead of a two-dimensional channel flow. Their measurements were confined to the mean velocity profiles, the longitudinal velocity fluctuations ($\overline{u'^2}$) and the spectrum of $\overline{u'^2}$. Laufer showed that during reverse transition in some regions the decay of $\overline{u'^2}$ is exponential and that the non-dimensional spectra of $\overline{u'^2}$ at the centre of the pipe exhibit complete similarity at all axial stations and the spectrum is exponential in wave-number. Sibulkin's experiments also indicated the similarity in the spectrum of $\overline{u'^2}$ and he noticed that the angle of the diffuser had no effect on the overall decay process, except for a short distance near its downstream end.

The aim of the present investigation is to study in greater detail the reverse transition process in a two-dimensional channel flow. The experiments were carried out with the following objectives: (*a*) to find out the critical Reynolds number for channel flow; (*b*) to measure the rate and mode of decay of the turbulent quantities; (*c*) to study the overall turbulent energy balance during decay; (*d*) to measure the spectrum of $\overline{u'^2}$ to find out whether similarity exists.

The accuracy of the measurements is not high due to the low mean velocities and low frequency fluctuations involved in the flow. The output readings were averaged over reasonably long periods (15–20 min) to obtain consistent results. The results show, with all the shortcomings, some definite and consistent trends and throw some light on the mechanism of the reverse transition process.

2. Experimental set-up

2.1. *Two-dimensional channel*

The geometry of the two-dimensional channel used for the investigation is shown in figure 1. The basic difficulty with this experimental investigation is the restricted height of the channel required to obtain sufficiently high velocities at low Reynolds numbers for accurate hot-wire measurements. It was decided that a two-dimensional channel having a width of $\frac{1}{2}$ in. is the most convenient size for

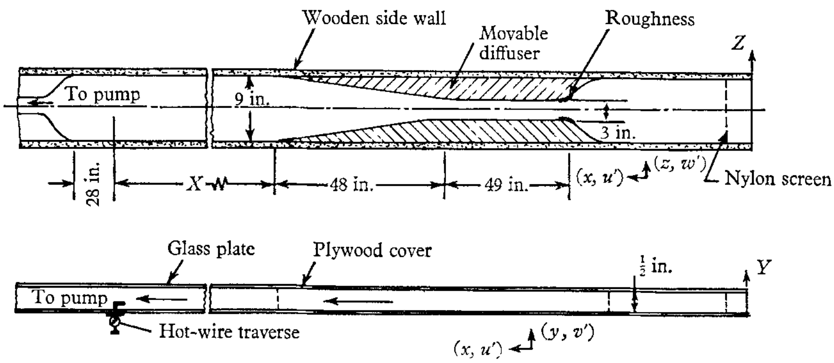

FIGURE 1. Diagram of the two-dimensional channel flow. (Not to scale.)

the experiment. Since both laminar and turbulent flows have to be obtained in the same set-up, the channel is made up of an initial narrow portion ($\frac{1}{2}$ in. high, 3 in. wide and 50 in. long) where the velocity is high and turbulent, and downstream of this a broad portion ($\frac{1}{2}$ in. high, 9 in. wide and 80 in. long) where the velocities and Reynolds numbers are low. A 3° half angle diffuser connected the two parallel sections of the channel. The complete channel was made of 1 in. thick plywood and the inner surface was polished very smooth, after being treated with Araldite resin. A suction pump was used to produce the flow in the channel. Strips of sand paper 6 in. long were pasted on each side of the channel at the entry region to hasten transition. Static pressure holes were drilled 6 in. apart along the channel and a sensitive manometer was used to measure differential pressures to an accuracy of 0·005 mm of water. In the early stages of the experiment, the diffuser was kept fixed and the hot wire was shifted from station to station along the channel. This method proved to be cumbersome and resulted in large scatter of the readings due to repeated shifting of the hot wire. It was later found more convenient to keep the hot wire fixed at one station (x) and to move the diffuser (see figure 1) along the channel.

2.2. *Hot-wire measurements*

The mean velocity and $\overline{u'^2}$ measurements were made using 0·0001 in. diameter platinum wire approximately 1 mm long. For cross wires, i.e. for $\overline{v'^2}$ and $\overline{u'v'}$ measurements, 0·0001 in. diameter platinum wires $\frac{1}{2}$ mm long were employed. A constant current anemometer system was used for the turbulence measurements. The hot-wire bridge and the amplifier were built in the laboratory. The circuit of the amplifier is the same as that of Townsend (1947) at the Cavendish

Laboratory except for some minor modifications. The amplifier had an overall gain of nearly 6000. Because the low-frequency fluctuations were quite large, the output readings had to be averaged over a long time to get reasonably repeatable results. The spectrum of $\overline{u'^2}$ was measured using a general electric wave analyser having a lower frequency limit of 2 c/sec. The hot wires were calibrated in a separate tunnel built for this purpose.

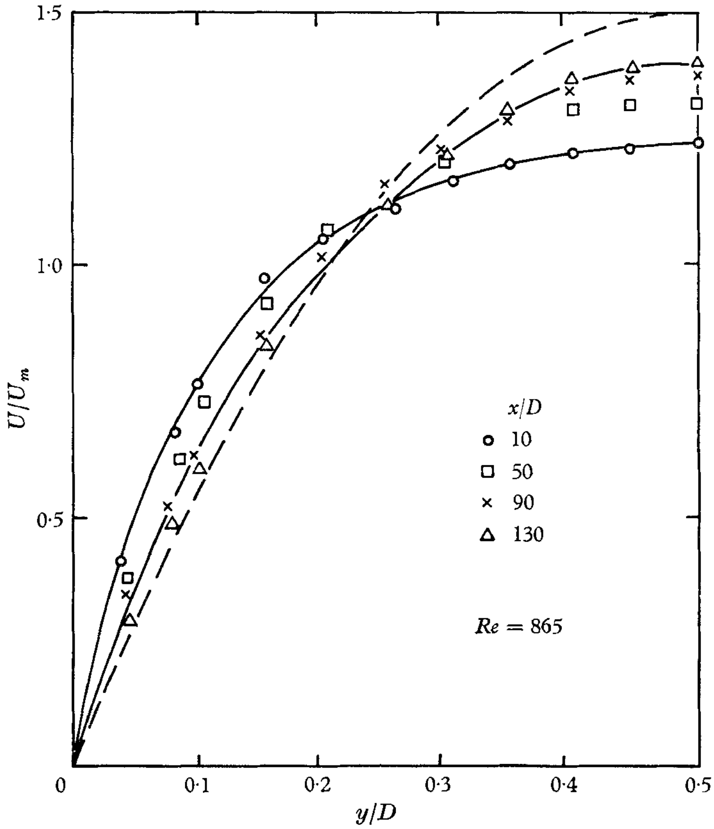

FIGURE 2. Mean velocity distributions at various axial stations. — — —, theoretical laminar profile.

3. Experimental results and discussion

In the region upstream of the diffuser some of the fluctuating quantities ($\overline{u'^2}$, $\overline{v'^2}$ and $\overline{u'v'}$) and mean velocities were measured to make sure that the flow was fully turbulent before being subjected to reverse transition process. The results indicated that the flow was reasonably fully developed and the mean velocity profiles when plotted in the universal logarithmic form, using wall shear values obtained from pressure gradient measurements, showed a definite logarithmic region and the wake component was practically negligible.

3.1. *Mean velocity profiles in the reverse transition region*

The mean velocity profiles downstream of the diffuser were measured at many axial stations (x) along the length of the channel at Reynolds numbers of 625, 865, 980 and 1250 based on half the channel height and the average of the mean

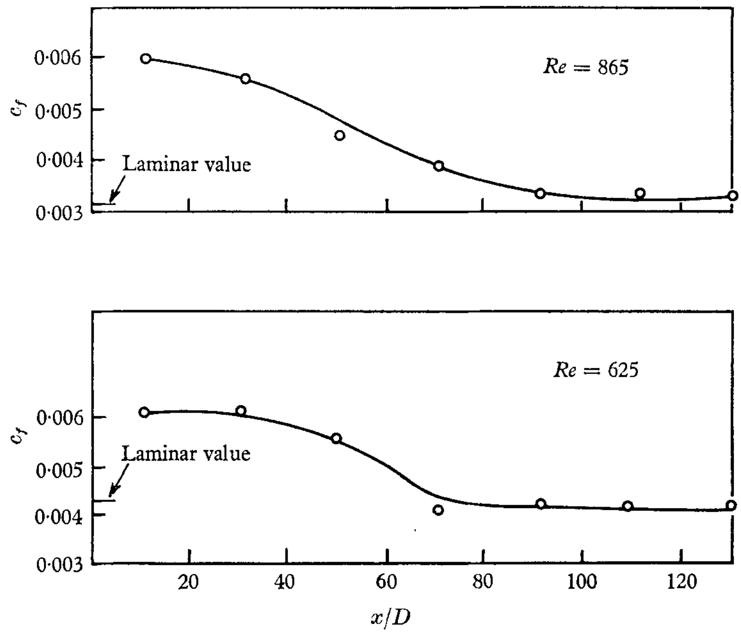

FIGURE 3. Variation of C_f along x_1 during inverse transition.

velocity (U_m). It was noticed that in each experiment hot-wire measurements showed that the average velocity (U_m) did not vary more than 5 % with x, and hence for practical purposes the Reynolds number is taken to be constant all along x in the reverse transition region. The velocity profiles for the case of $Re = 865$ are shown in figure 2. The mean velocity profiles show a tendency to become laminar as the flow moves downstream and this change is more rapid as the Reynolds number decreases. The estimated values of the skin friction coefficients (c_f) obtained from static pressure and mean velocity measurement show a decrease in the value of c_f (figure 3) during reverse transition. The flow field being not invariant with respect to x the change in momentum due to the mean velocity variation is also taken into account in the evaluation of c_f. At Reynolds number of 625 and 865, the value of c_f reached that of laminar flow much earlier, even though the mean velocity profiles in the outer region have not reached similar conditions, indicating that the history of the flow is retained more in the outer region than in the inner region.

3.2. *Turbulent quantities*

The turbulent quantities $\overline{u'^2}$, $\overline{v'^2}$ and $\overline{u'v'}$ were measured at all the four reverse transition Reynolds numbers and the measured profiles are shown in figures 4–6 for the case of Re 865. Due to the finite thickness of the hot-wire probes, $\overline{v'^2}$ and

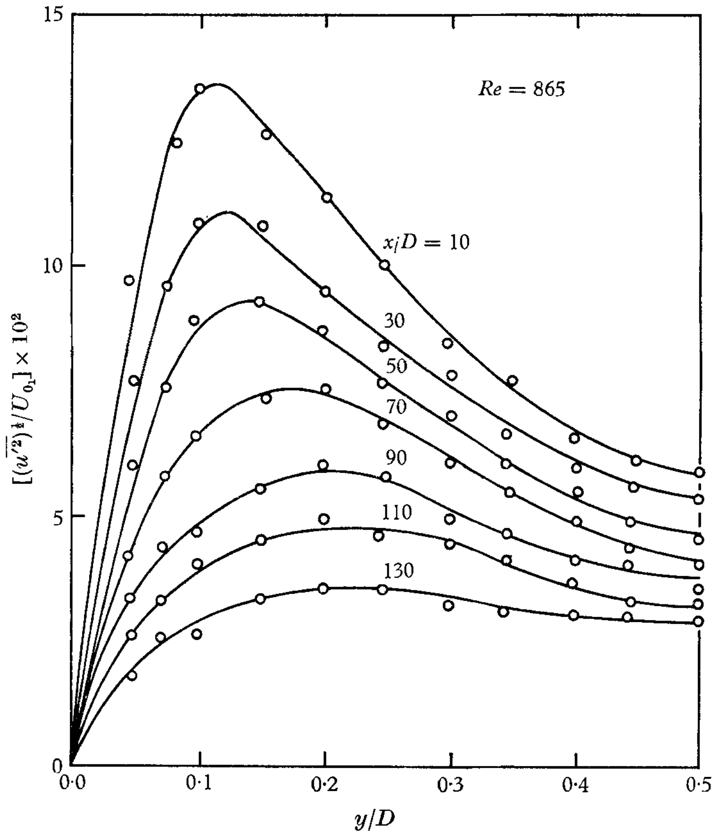

FIGURE 4. Distributions of $\overline{u'^2}$ across the channel at various axial stations.

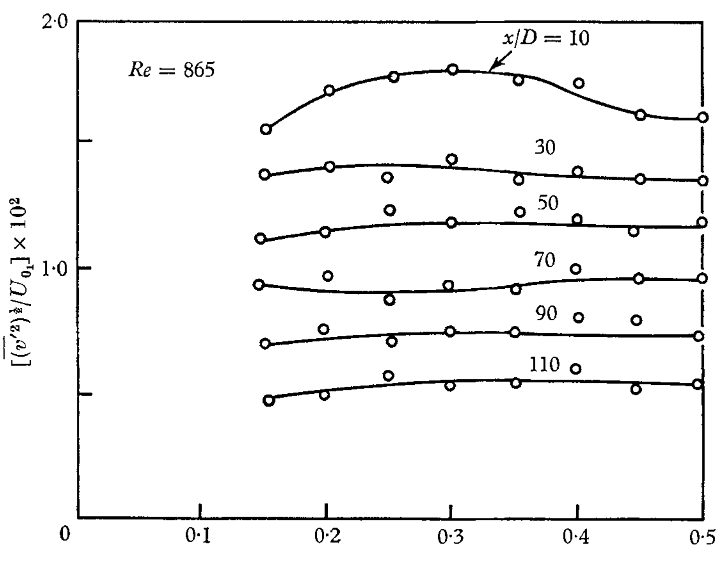

FIGURE 5. Distributions of $\overline{v'^2}$ across the channel at various axial stations.

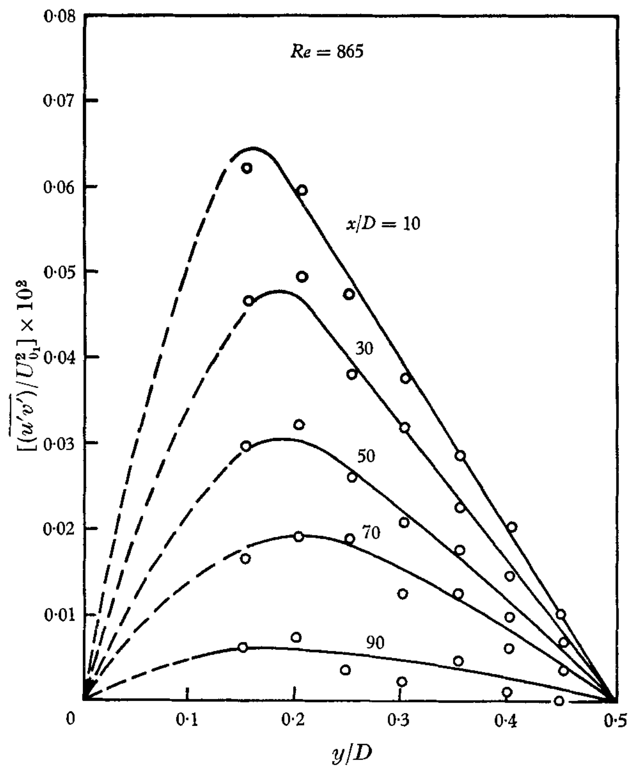

FIGURE 6. Distribution of $\overline{u'v'}$ across the channel height.

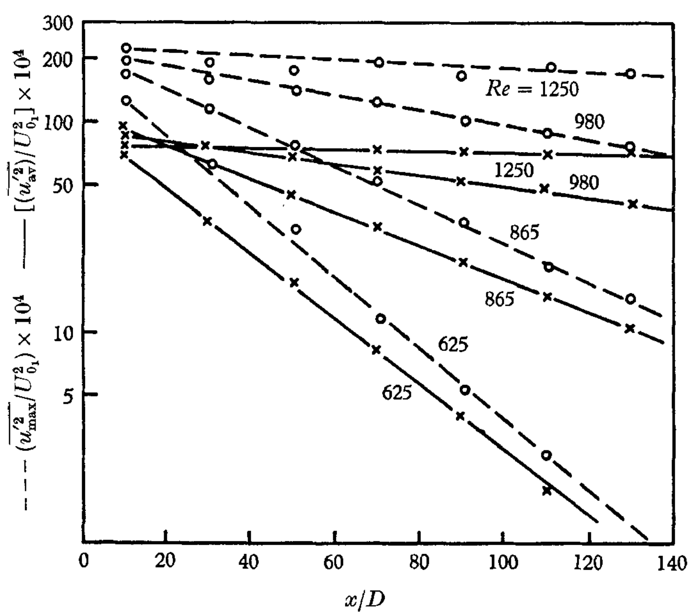

FIGURE 7. Decay of $\overline{u'^2_{max}}$ and $\overline{u'^2_{av}}$ along the channel. – – –, $\overline{u'^2_{max}}$; ——, $\overline{u'^2_{av}}$.

$\overline{u'v'}$ could not be measured very close to the wall, and in figure 6 the $\overline{u'v'}$ curve has been extrapolated to the wall (dotted line). The values of the fluctuating quantities decrease as the flow moves downstream and there is a shift in the position (y/D) of the peaks of $\overline{u'^2}$ and $\overline{u'v'}$ towards the channel centre during the reverse transition process. The average value of $\overline{u'^2}$ obtained by integrating $\overline{u'^2}$ across the channel height exhibits an exponential decay with respect to x (figure 7), indicating that the overall decay process is essentially exponential unlike the case of isotropic turbulence where the decay is proportional to $1/x$ in the initial region. The maximum value of $\overline{u'^2}$ also shows an exponential decay (figure 7). But this exponential decay is not maintained at all layers (y/D) except near the wall and the channel central regions. A similar trend has been noticed by Laufer also during his investigation of reverse transition in pipe flow.

During the reverse transition process the location of $\overline{u'^2}$ shifts away from the wall, as the flow moves downstream. If the distance between the wall and the location of $\overline{u'^2_{\max}}$ is taken as the characteristic length scale (α), the decay of $\overline{u'^2}$ becomes exponential at all (y/D) layers. Using the length scale (α) and the $\overline{u'^2_{\max}}$ (as the velocity scale) it is now found possible to collapse all the $\overline{u'^2}$ curves on to a single one (figure 8). This result indicates that there is some kind of near similarity in the decay process.

The decay of $\overline{v'^2}$ along the centre of the channel is again exponential (figure 9) and since the gradients in the y-direction are small the overall decay also should be exponential as in the case of $\overline{u'^2}$. The $\overline{v'^2}$ profiles also exhibit similarity when the same velocity and length scales used in conjunction with $\overline{u'^2}$ are employed. The decay curves show that $\overline{v'^2}$ decreases faster than $\overline{u'^2}$. For example, the ratio of $\overline{u'^2}/\overline{v'^2}$ which is around 16 at $x/D = 10$ for $Re = 865$, increases to a value of 36 at $x/D = 110$, and the increase is more (200) at the lower $Re = 625$. $\overline{w'^2}$ could not be measured accurately due to the small size of the channel. The mean velocity itself was appreciably affected when the hot-wire probe was oriented for w' measurements. But some crude measurements made at a few stations indicated $\overline{w'^2}$ to be of the same magnitude as that of $\overline{v'^2}$. Since $\overline{u'^2}$ is much larger than $\overline{v'^2}$ and hence $\overline{w'^2}$, the errors involved in the estimation of the total turbulent kinetic energy will not be more than 6 %, even if the error in the measurement of $\overline{w'^2}$ is of the order of 50 %.

The $\overline{u'v'}$ profiles indicate that the turbulent shear stress varies linearly with y for some distance near the centre of the channel and then drops towards zero as the wall region is approached. To study the rate of decay, values of $\overline{u'v'}$ at $y/D = 0{\cdot}25$ are taken for comparison. The decay of $\overline{u'v'}$ with x seems linear (figure 10) instead of being exponential as in the cases of $\overline{u'^2}$ and $\overline{v'^2}$. This result was somewhat unexpected and in addition $\overline{u'v'}$ decays earlier and approaches zero value before other turbulent quantities vanish. It is also interesting to note that $\overline{u'v'}$ becomes zero at the same x region where the wall shear drops to laminar value (see figure 3). No similarity exists in the $\overline{u'v'}$ distribution when the same length and velocity scales used in connexion with $\overline{u'^2}$ and $\overline{v'^2}$ are employed. During the reverse transition process there seems to be decoupling between the u' and v' fluctuation because measured correlation coefficients $\overline{u'v'}/(\overline{u'^2})^{\frac{1}{2}}(\overline{v'^2})^{\frac{1}{2}}$, indicate a gradual decrease in the correlation (figure 11) as the flow moves downstream. Lissajous figures obtained by feeding u' and v' signals to an oscilloscope (long exposure) also show a similar trend. The above results definitely support the view that the u' and v' fluctuations are getting uncorrelated during the reverse transition process.

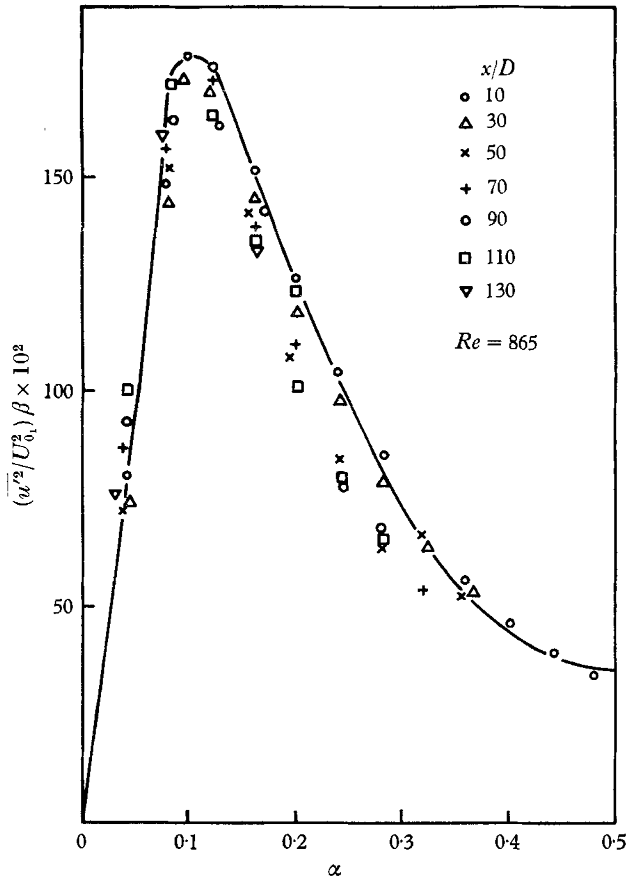

FIGURE 8. Similarity in $\overline{u'^2}$ profiles.

$$\alpha = y/L\frac{y \text{ at } \overline{u'^2_{\max}} \text{ at } x/D = 10}{y \text{ at } \overline{u'^2_{\max}}}, \quad \beta = \frac{\overline{u'^2_{\max}} \text{ at } x/D = 10}{\overline{u'^2_{\max}}}.$$

3.3. *Turbulent spectrum*

The spectrum of $\overline{u'^2}$ was measured along the centreline of the channel ($y/D = 0{\cdot}5$) at three axial stations at $R = 865$. The non-dimensional spectrum is shown in figure 12. The measurements show that there is complete similarity at all the three stations during the decay process. Similar trend had been noticed by Laufer (1962) and Sibulkin (1962) during reverse transition in pipe flow. They have shown that the spectrum follows roughly the curve given by

$$\frac{F_u(k)}{L_x} = \frac{2}{\pi}\exp\{-(2/\pi K L_x)\},$$

where L_x is the integral length scale, k is the wave-number. In the present investigation also the same relation seems to hold good. This similarity of the spectrum during the reverse transition process is somewhat surprising since the relation between wave number and the spectrum is not very clear even in the case of isotropic turbulence except possibly at high wave numbers. But during inverse transition one would expect the problem to be more complicated since the Reynolds numbers are low and the energy transfer process from the various eddy sizes are unknown. But, on the other hand, there is almost perfect similarity

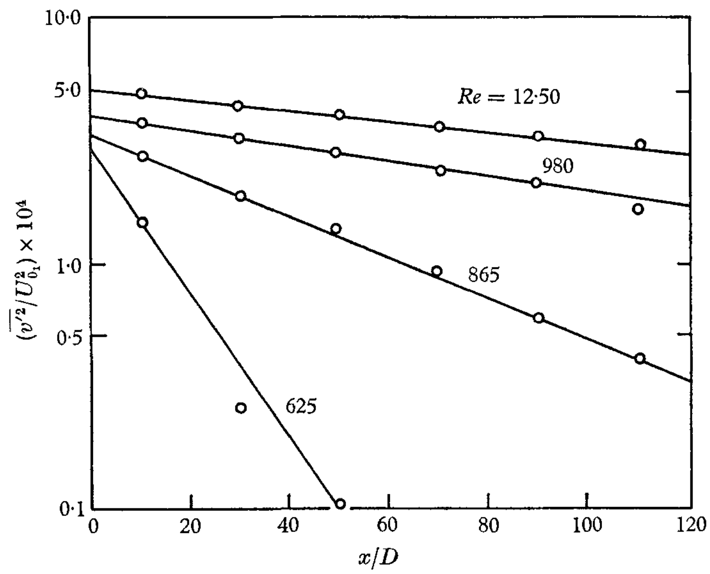

FIGURE 9. Decay of $\overline{v'^2}$ (at $y/D = 0{\cdot}5$) along the channel axis.

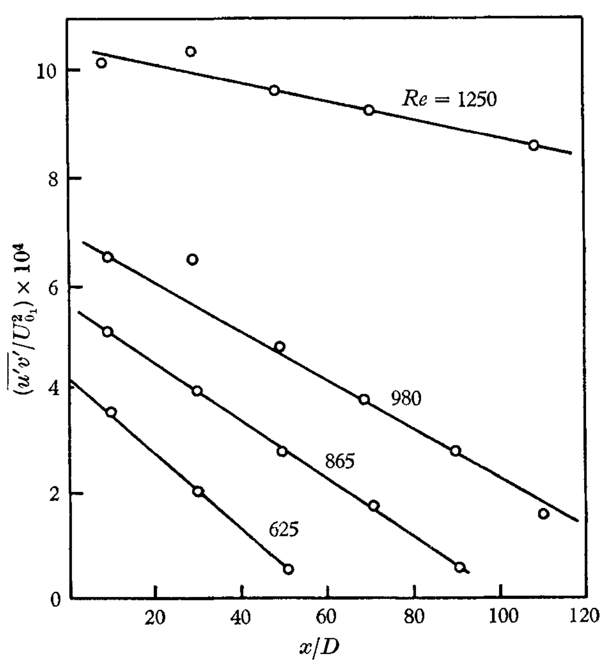

FIGURE 10. Variation of $\overline{u'v'}$ along the channel. Shear measured at $y/D = 0{\cdot}25$.

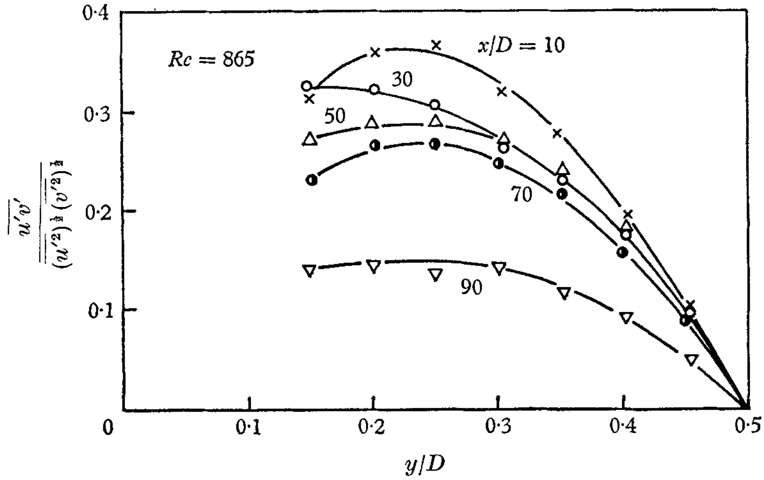

FIGURE 11. Correlation coefficient distribution.

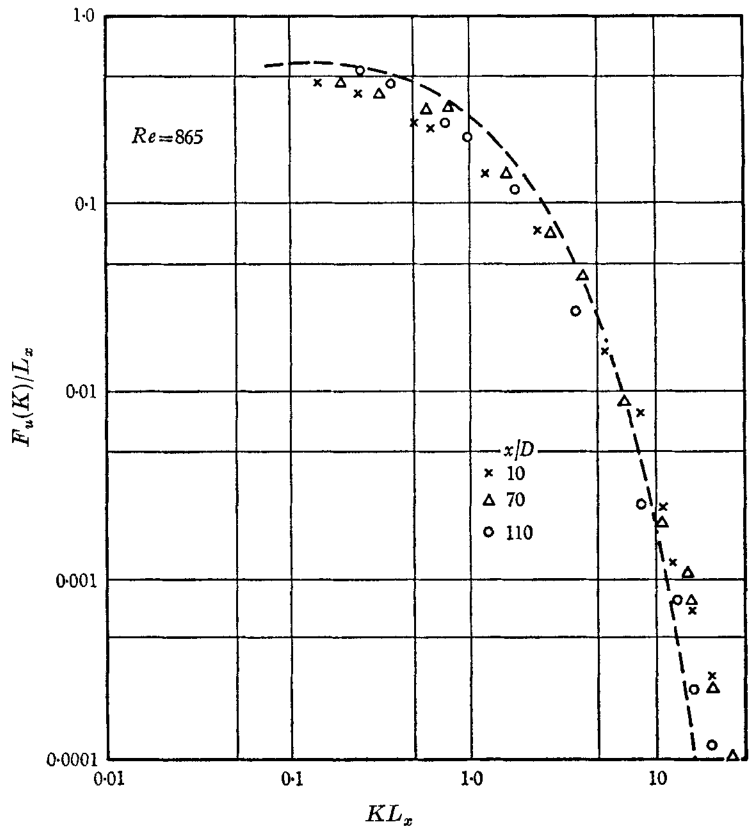

FIGURE 12. Spectra along the centre line of the channel. – – –, $F_u(K)/L_x = (2/\pi)\, e^{-2/\pi K L_x}$.

and this trend suggests some kind of local equilibrium in the flow. This view is supported to some extent by the near similarity in the $\overline{u'^2}$ and $\overline{v'^2}$ profiles observed during the decay process.

The integral scale L_x $(=[2/\pi]\,F_u(0))$, and the microscale λ_x, given by the equation

$$\frac{1}{\lambda x^2} = \frac{1}{2}\int_0^D k^2 F_u(k)\,dk$$

as obtained from the spectrum measurements are tabulated below:

x/D	λ_x/D	L_x/D
10	0·72	1·7
70	1·18	2·35
110	1·56	2·90

(Measured at y/D = 0·5 and at Re = 865.)

The microscale as well as the integral scale are comparable with the height of the channel (D) and the latter is in fact larger than D at all stations downstream of the diffuser.

3.4. *Critical Reynolds number*

The critical Reynolds number for reverse transition is estimated on the assumption that the decay rates for all the fluctuating quantities should tend to zero

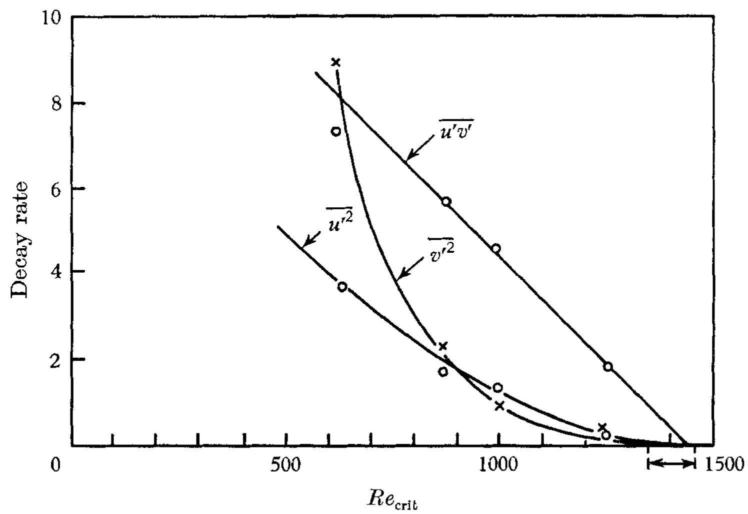

FIGURE 13. Determination of critical Reynolds number.

as this Reynolds number is approached. When the slopes of $\overline{u'^2}$, $\overline{v'^2}$ and $\overline{u'v'}$ (figures 7, 9 and 10) are plotted against Reynolds number, the curves (figure 13) tend to zero simultaneously around a Reynolds number of 1400 ± 50 and this seems to be at present the best method for the evaluation of the critical Reynolds number for reverse transition.

3.5. *Turbulent energy balance*

The complete turbulent energy equation is given by (Corrsin 1953)

$$U_l\frac{\partial\overline{q'^2}}{\partial x_l}+2\,\overline{u_i'u_l'}\frac{\partial U_i}{\partial x_l}+\frac{\partial\overline{q'^2u_l'}}{\partial x_l}=-\frac{2}{\rho}\frac{\partial\overline{p'u_l'}}{\partial x_l}+\nu\frac{\partial^2\overline{q'^2}}{\partial x_i\partial x_i}-2\nu\frac{\overline{\partial u_i'\partial u_i'}}{\partial x_l\partial x_l},\qquad(1)$$

where $\overline{q'^2}=\overline{u'^2}+\overline{v'^2}+\overline{w'^2}$ and p' is the fluctuating pressure. In this equation, the last two terms give the total turbulent energy transported and dissipated by viscosity but do not represent them individually, unless the Reynolds number is high, where viscous effects are predominant only in the small eddy level. This assumption is highly questionable at low Reynolds numbers. In this report for convenience the two terms are called viscous diffusion and isotropic dissipation respectively.

By using the following assumptions, relevant to this particular flow, the number of terms in (1) is considerably smaller.

(i) The mean velocity component V is small compared to U since the profiles change their shape slowly.

(ii) The mean velocity W is zero due to two-dimensionality of the flow.

(iii) There are no gradients in the Z-direction.

(iv) $\overline{w'^2}$ is approximately equal to $\overline{v'^2}$ in magnitude.

(v) The gradients of $\overline{q'^2}=\overline{u'^2}+\overline{v'^2}+\overline{w'^2}$ are larger in the y-direction than in the x-direction.

With these basic assumptions, equation (1) reduces to:

$$U\frac{\partial\overline{q'^2}}{\partial x}+2\overline{u'v'}\frac{\partial U}{\partial y}+\frac{\partial\overline{q'^2v'}}{\partial y}=\frac{2}{\rho}\frac{\partial\overline{p'v'}}{\partial y}+\nu\frac{\partial^2\overline{q'^2}}{\partial y^2}-2\nu\overline{(\partial u_i'/\partial x_l)(\partial u_i'/\partial x_l)}.\qquad(2)$$

In the above equation (2) the terms represent respectively advection of turbulent energy along the mainstream, production of turbulence, turbulent convection, convection due to pressure fluctuations, turbulent energy transfer due to viscosity and dissipation of turbulence into heat respectively. Estimation of all these terms is rather difficult since it calls for elaborate measurements. An integral approach is used in the present investigation. When the energy equation (2) is integrated across half the width of the channel, it reduces to the form,

$$\int_0^{\frac{1}{2}D}U\frac{\partial\overline{q'^2}}{\partial x}dy+2\rho\int_0^{\frac{1}{2}D}\overline{u'v'}\frac{\partial U}{\partial y}dy=2\mu\int_0^{\frac{1}{2}D}\overline{(\partial u_i'/\partial x_l)(\partial u_i'/\partial x_l)}\,dy.\qquad(3)$$

(The term $\int_0^{\frac{1}{2}D}\frac{\partial^2\overline{q'^2}}{\partial y^2}dy$ is found to be very small.)

According to this equation the overall advection and production is balanced by dissipation. With the help of the present measurements, it is possible to calculate the first two terms and the sum of these two terms should be dissipation. The results are plotted in figure 14. The advection is relatively small throughout the flow and it looks as though production and dissipation nearly balance each other. This trend suggests the possibility of some kind of local equilibrium in the flow during the reverse transition process and this idea is also supported to some extent by the similarity in $\overline{u'^2}$ profiles and the spectrum of $\overline{u'^2}$.

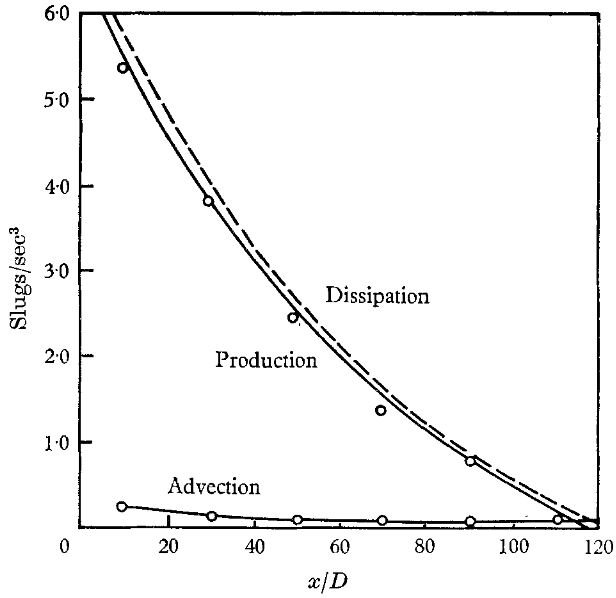

FIGURE 14. Variation of integrated turbulent energy along the channel.

4. Conclusions

The fluctuating turbulent quantities, as well as the mean velocity profiles, indicate that the decay distance (x) for reverse transition increases with Reynolds number. The mean velocity profiles show that the wall region adjusts itself to laminar conditions earlier than the outer region. The decay rates of the fluctuating quantities ($\overline{u'^2}$, $\overline{v'^2}$, $\overline{u'v'}$) when plotted against Reynolds number show that the rates tend to zero simultaneously for all the fluctuating quantities at a definite Reynolds number of 1400 ± 50 indicating that this is the critical Reynolds number for reverse transition in channel flow. The decay of $\overline{u'^2}$ (average) is exponential with x, but in detail, the laws of decay are different at different layers (y/D). The decay of $\overline{v'^2}$ (average) is also exponential. Though the rates and laws of decay of $\overline{u'^2}$ are different at different layers (y/D), there is approximate similarity in the $\overline{u'^2}$ profiles if the maximum value of $\overline{u'^2}$ and its location (y/D) are taken as the characteristic velocity and length scales. $\overline{v'^2}$ also exhibits similarity. The turbulent shear stress $-\rho\overline{u'v'}$ measurements show that the distribution of $\overline{u'v'}$ is linear in the outer region of the flow and in this region the decay of $\overline{u'v'}$ with respect of x is almost linear. At some distance x, $\overline{u'v'}$ becomes zero when $\overline{u'^2}$ and $\overline{v'^2}$ are still finite. Beyond this region, the flow can be considered to be just disturbed laminar flow. The correlation coefficient $\overline{u'v'}/(\overline{u'^2})^{\frac{1}{2}}(\overline{v'^2})^{\frac{1}{2}}$ also decreases during reverse transition and this fact is supported by Lissajous figures obtained with u' and v' signals. $\overline{u'^2}$ spectrum show almost perfect similarity along the central line of the channel and the spectrum function is nearly exponential in wave-number. The turbulent energy when integrated across the height of the channel shows that the dissipation is almost balanced by production, indicating some kind of local equilibrium in the flow. This idea is supported to some extent by the similarity in $\overline{u'^2}$ profiles and the spectrum.

The author thanks Dr Satish Dhawan for the encouragement and advice given during the course of the work. Dr Roddam Narasimha has spent a great deal of time discussing with me in detail many aspects of the problem, in particular the analysis regarding the decay of the turbulence and the critical Reynolds number was suggested by him. Thanks are due to Prof. H. W. Liepmann who during his visit to the Institute spent a considerable amount of his precious time in the final discussions and made many illuminating comments.

REFERENCES

BATCHELOR, G. K. 1959 *The Theory of Homogeneous Turbulence.* Cambridge University Press.

CORRSIN, S. 1953 Interpretation of viscous terms in the turbulent energy equation. *J. Aero. Sci. Readers Forum*, **20**, 853–854.

HOLDER, D. W., GADD, G. E. & REGAN, J. D. 1956 Base pressures in supersonic flow. C.P. no. 271.

LAUFER, J. 1962 Decay of nonisotropic turbulent field. *Mitteilungen der Angewandten Mechanik*, pp. 166–74. Edited by Manfred Schaefer. Gottingen.

LAUNDER, B. E. 1964 Laminarization of the turbulent boundary layer in a severe pressure gradient. *Trans. ASME* (*J. Appl. Mech.*).

MORETTI, P. M. & KAYS, W. M. 1965 Heat transfer to a turbulent boundary layer with varying free-stream velocity and varying surface temperature—an experimental study. *Int. J. Heat Mass Transfer*, **8**, 1187–1202.

SERGIENKO, A. A. & GRETSOV, V. K. 1959 Transition from turbulent to laminar boundary layer. *Dokl. Akad. Nauk, SSSR*, 746 (1959) 125.

SIBULKIN, M. 1962 Transition from turbulent to laminar flow. *The Physics of Fluids*, **5**, 280–289.

STERNBERG, J. 1954 The transition from turbulent to laminar boundary layer. *U.S. Army Bal. Res. Lab. Rept.* no. 906.

TOWNSEND, A. A. 1947 The measurement of double and triple correlation derivatives in isotropic turbulence. *Proc. Cambridge Phil. Soc.* **43**, 560.